Atmos. Chem. Phys. Discuss., 7, 9795–9828, 2007
www.atmos-chem-phys-discuss.net/7/9795/2007/

Atmospheric Chemistry and Physics Discussions

Tropospheric ozone climatology over Beijing: analysis of aircraft data from the MOZAIC program

A. J. Ding[1], T. Wang[1], V. Thouret[2], J.-P. Cammas[2], and P. Nédélec[2]

[1]Department of Civil and Structural Engineering, The Hong Kong Polytechnic University, Hong Kong, China
[2]Laboratoire d'Aérologie, UMR 5560, Université Paul Sabatier, Toulouse, France

Received: 23 May 2007 – Accepted: 21 June 2007 – Published: 5 July 2007

Correspondence to: T. Wang (cetwang@polyu.edu.hk)

Abstract

Ozone (O_3) profiles recorded over Beijing from 1995 to 2005 by the Measurement of Ozone and Water Vapor by Airbus In-Service Aircraft (MOZAIC) program were analyzed to provide a first climatology of tropospheric O_3 over Beijing and the North China Plains (NCPs), one of the most populated and polluted regions in China. A pooled method was adopted in the data analysis to reduce the influence of irregular sampling frequency. The tropospheric O_3 over Beijing shows a seasonal and vertical distribution typical of mid-latitude locations in the Northern Hemisphere, but has higher daytime concentrations in the lower troposphere, when compared to New York City, Tokyo, and Paris at similar latitude. The tropospheric O_3 over Beijing exhibits a common summer maximum and a winter minimum, with a broad summer maximum in the middle troposphere and a narrower early summer (June) peak in the lower troposphere. Examination of meteorological and satellite data suggests that the lower tropospheric O_3 maximum in June is a result of strong photochemical production, transport of regional pollution, and possibly also more intense burnings of biomass in Central-Eastern China. Trajectory analysis indicates that in summer the regional pollution sources from the NCPs, maybe mixed with urban plumes from Beijing, played important roles on the high O_3 concentrations in the boundary layer, but had limited impact on the O_3 concentrations in the middle troposphere. A comparison of the data recorded before and after 2000 reveals that O_3 in the lower troposphere over Beijing had a strong positive trend (approximately 2% per year from 1995 to 2005) in contrast to a flat or a decreasing trend over Tokyo, New York City, and Paris, indicating worsening photochemical pollution in Beijing and the NCPs.

1 Introduction

Ozone (O_3) is a key trace gas in the troposphere owing to its important roles in atmospheric chemistry, air quality, and climate change. O_3 determines the oxidizing capacity

ACPD

7, 9795–9828, 2007

of the atmosphere through generation of the principal oxidizing agent, hydroxyl radical (OH), and it is also an effective greenhouse gas in the upper troposphere (Crutzen, 1973; Fishman et al., 1979; Bojkov, 1988). High concentrations of O_3 at ground level is of great concern because of its harmful effects on human health and vegetation (Mckee, 1994; NRC, 1991). Therefore, the temporal and spatial distribution of tropospheric O_3 and the factors controlling its distribution has been a focus of atmospheric chemistry research.

While numerous studies were conducted in Europe, North America, and in Japan (Beekmann et al., 1994; Logan, 1985, 1994; Liu et al., 1987; Oltmans et al., 1998; Monks, 2000; Akimoto et al., 1994; Pochanart et al., 2002), there is limited knowledge of the temporal and spatial distribution of tropospheric O_3 on the Chinese subcontinent where rapid urbanization and industrial developments have been taken place in the latest two decades. Previous studies of emissions have projected sharp increases in the emissions of O_3 precursors in China, especially in the fastest growing coastal regions of eastern China (Akimoto and Narita, 1994; Streets et al., 2003). Recently available satellite data have shown an increasing column concentrations of nitrogen dioxide, a precursor to O_3, over China (Richter et al., 2005). Available ground-based measurements within China have shown frequent O_3 pollution during photochemically active seasons in sub-urban and rural areas of these regions (e.g. Cheung and Wang, 2001; Wang and Kwok, 2003; Gao et al., 2005; Wang et al., 2006a). Seasonal cycles of surface ozone were reported at Lin'an in eastern China (Wang et al., 2001; Luo et al., 2000; Xu et al. , 2007), a coastal background site (Hok Tsui) and a suburban site (Tai O) in Hong Kong (Lam et al., 2001; Wang et al., 2005), a rural site (Shangdianzi) near Beijing (Liu et al., 2006), and three mountaintop sites (Mount Tai, Mount Hua, and Mount Huang)[1].

Monthly mean O_3 concentration was found to reach a maximum in early summer

[1]Li, J., Wang, Z. F., Akimoto, H., Gao, C., Pochanart, P., and Wang, X.: Modeling study of the seasonal cycle of ozone in the boundary layer over East Asia, J. Geophys. Res., in review, 2007.

(May or June) in central and eastern China and in autumn in southern China. Vertical distribution of O_3 in the troposphere over China has been examined using ozonesondes which were launched mainly during intensive campaigns (Chan et al., 2003; Zheng et al., 2004). Using satellite data from GOME (Global Ozone Monitoring Experiment), Fishman et al. (2003) showed higher tropospheric O_3 residual in eastern China than in other mid-latitude regions of the Northern Hemisphere. Nevertheless, additional data on O_3 are needed in many parts of China, particularly the data that give vertical distribution and long-term trend of tropospheric O_3.

In this study we analyze O_3 profiles obtained during 1995–2005 by the Measurement of Ozone and Water Vapor by Airbus In-Service Aircraft (MOZAIC) Program (http://mozaic.aero.obs-mip.fr) to investigate the climatology of tropospheric O_3 distribution over Beijing. Since 1994, O_3 and other trace gases have been routinely measured on board commercial airliners flying between large cities around the world, including three mega-cities in China: Beijing, Shanghai, and Hong Kong. This program has generated a unique dataset for studying tropospheric O_3. In this work, we focus on the O_3 distribution over Beijing and the surrounding areas for the following reasons. First, this region is one of the most polluted parts of China. For instance, 200–300 ppbv of O_3 has been reported in urban and rural areas of Beijing (Shao et al., 2006; Wang et al., 2006a). Second, Beijing will host the 2008 Summer Olympics; poor air quality (including summertime photochemical O_3 pollution) is of a paramount concern of the central and municipal governments. Third, in China MOZAIC data have been collected over the longest period in Beijing. We examine the temporal and vertical distributions of O_3 and the trend during 1995–2005, and with aid of meteorological and satellite data we discuss the role of emission, dynamic transport, and photochemistry.

2 Data and methodologies

2.1 MOZAIC O_3 data over Beijing

The Measurement of Ozone and Water Vapor by Airbus In-Service Aircraft (MOZAIC) program has been designed to routinely observe O_3 and water vapor along flight routes using automatic instruments installed onboard commercial airliners flying regularly all over the world (Marenco et al., 1998). O_3 was measured using the dual-beam UV absorption analyzer (Thermo Environment Instruments – Model 49–103), with an overall measurement precision of ±2 ppbv. The sensors were recalibrated after every 500 flight hours (Thouret et al., 1998a, 2006). More details of this program can be found on the MOZAIC website (http://mozaic.aero.obs-mip.fr).

In the present study, we mainly draw on O_3 profiles recorded in the ascent and descent stages of the flights during 1994–2005 over Beijing and three other mega-cities in the northern mid-latitudes: New York City, Tokyo, and Paris. The raw MOZAIC data have a temporal resolution of 4 s, i.e. about 30 m vertically. We use the reproduced data with a vertical resolution of 250 m below 2 km and 500 m above 2 km. For Beijing, there were about 800 profiles taken by this program from March 1995 to August 2005. In other mega-cites, more profiles (about 1300, 4400, and 3300 for Tokyo, Paris, and New York, respectively) were obtained during 1994–2005.

Figure 1a gives the geographical coverage of the MOZAIC flight routes around Beijing on a topographical and land-use map, and Figs. 1b and 1c show the distribution of the number of profiles as a function of month and the local time of day, respectively. From Fig. 1a, it can be clearly seen that Beijing is located on the north side of the North China Plains (NCPs), and the Beijing Capital International Airport sits northeast to the urban center with a distance of about 25 km. Both urban Beijing and the airport are embraced by mountains in the west, north and northeast, with heights ranging from several hundreds meters to 2 km. Figure 1a also shows that the MOZAIC aircraft descended and ascended along relatively fixed routes, circling near the airport on the east side. We used the data collected within a box of 3 by 3° in longitude/latitude (115.5–118.5° E,

39.0–42.0° N) with Beijing in the center of the box (see the blue dashed box in Fig. 1a). Figure 1b shows that there was large year-to-year difference in the number of profiles recorded, with more data collected during 1997–1998 and around 2005. Figure 1c shows that most of the profiles over Beijing were taken in the daytime (05:00–17:00, local time (LT)). Other cities may have different diurnal distributions of sample numbers; in New York City, for example, most of profiles were taken within 10:00–23:00 LT (Thouret et al., 1998b).

2.2 Meteorological and satellite data, and trajectory calculation

To help interpret the MOZAIC O_3 profiles, we use various meteorological and satellite data, and back trajectories. A brief description of these data and products is given below.

The meteorological data include twice-a-day (00:00 and 12:00 Greenwich time) radiosonde data, surface wind and rainfall data measured at Beijing Observatory (from CISL at NCAR, http://dss.ucar.edu/datasets/), monthly mean sunshine hours and rainfall data at Beijing (Chinese Statistical Yearbook 1996–2006, http://www.stats.gov.cn/tjsj/ndsj/), and monthly mean NCEP/NCAR reanalysis data, with a resolution of 2.5° in latitude and longitude (from NOAA CDC, http://www.cdc.noaa.gov/cdc/).

Two kinds of satellite data were used to provide the regional perspective of air pollutants. One is the monthly mean global tropospheric NO_2 column, with a 0.5 degree resolution, obtained by GOME (Global Ozone Monitoring Experiment, 1995–2002) and SCIAMACHY (SCanning Imaging Absorption spectroMeter for Atmospheric CHartography, 2003-present) (data were obtained via TEMIS, http://www.temis.nl/index.html). Another one is the nighttime fire count product retrieved from ATSR-2 (Along Track Scanning Radiometer 2) using Algorithm#2 (http://dup.esrin.esa.int/ionia/about_ionia.asp).

To help understand the influence of long-range transport on the vertical distribution of tropospheric O_3, we calculated back-trajectories using HYSPLIT (HYbrid Single-Particle Lagrangian Integrated Trajectory, version 4.8) model of NOAA Air Resources

Laboratory (http://www.arl.noaa.gov/ready/hysplit4.html). The FNL data with a horizontal resolution of about 190 km were used to drive the model.

2.3 Pooled statistical analysis

Vertical profiles from the aircraft survey provide "snapshots" of O_3 distribution for a relatively short period of time. As shown in Figs. 1b and 1c, the sampling frequency of MOZAIC O_3 profile is not evenly distributed seasonally and diurnally. Therefore the conventional averaging method may not truly represent the overall mean behavior of O_3, particularly in the lower troposphere where O_3 has strong seasonal and diurnal variations. In the present work we adopt a pooled statistical method introduced by Taylor and Cihon (2004).

The concept of pooled statistical analysis is to divide the data into several groups (of same season and/or of same time of day), and then pool their means and standard deviations (SDs) together. If the O_3 data at a certain height were defined as $\hat{X}$, we first divide them into N groups $\hat{X}_i$(i=1, 2... N), and then calculate the mean ($\bar{X}_i$) and SD (S_i) of each group. We then have the pooled average as:

$$\bar{X}_p = \frac{1}{N} \sum (\bar{X}_i). \quad (1)$$

and pooled SD as:

$$S_p = \sqrt{\frac{\sum S_i^2 \cdot (M_i - 1)}{\sum (M_i - 1)}}. \quad (2)$$

where M_i is the number of data points of the ith group. The value for S_p is based on degrees of freedom as

$$df_p = \sum (M_i - 1). \quad (3)$$

ACPD
7, 9795–9828, 2007

EGU

3 Results and discussions

3.1 Overall results over Beijing and a comparison with other cities

Figure 2 gives the vertical distributions of O_3 below 10 km using two different statistical methods: the conventional method (i.e. grand average) and the pooled method with data being divided into 36 groups (12 months ×3 periods of day (05:00–08:00 LT, 09:00–12:00 LT, and 13:00–16:00 LT)). It can be seen that the two methods give a very similar vertical distribution of O_3, with a difference of 1–2 ppbv in the mean values. However the SDs of the pooled method were obviously smaller, especially in the Planetary Boundary Layer (PBL). Given a decrease of 36 in degrees of freedom (from a total of 810 profiles), the pooled method should provide results with a larger statistical significance.

Figure 2 shows that the mixing ratio of O_3 increased from ~40 ppbv at ground to ~65 ppbv around 8 km, and then increased rapidly above 8 km with a larger variability near the tropopause. Such a mean O_3 distribution is typical for locations in mid-latitudes (Logan, 1994; Beekmann et al., 1994; Thouret et al., 1998b; Cooper et al., 2005). In the PBL the O_3 concentrations increased sharply below 1 km and then remained fairly constant (~52 ppbv) between 1 km and 2 km. This feature is mainly related to the diurnal cycle of PBL O_3, which will be further discussed in Sect. 3.2.

Figures 3a and 3b compare the lower tropospheric O_3 over Beijing with the profiles obtained over Tokyo, Paris, and New York City using non-pooled (Fig. 3a) and pooled method (Fig. 3b), respectively. For the pooled method, only data collected at the common daytime (10:00–14:00 LT) in the four cities were selected, and these data were divided into 20 groups (4 seasons ×5 h). Both Figs. 3a and 3b show the highest mean O_3 concentrations in the lower troposphere over Beijing, which is about 10 ppbv higher in the PBL according to the pooled method. This indicates that Beijing has higher tropospheric O_3 concentrations than those at mega-cities of the similar latitudes in Europe, Japan, and the eastern United States. This result is consistent with the work of Fishman et al. (2003) who showed higher tropospheric O_3 residual in eastern China

ACPD
7, 9795–9828, 2007

EGU

based on an analysis of GOME data.

3.2 Diurnal variation of lower tropospheric O_3

Figures 4a to 4c show mean diurnal patterns of O_3 from ground to 3.5 km altitude over Beijing for whole year, summer, and winter. The annual mean results (Fig. 4a) are pooled from data collected in the four seasons (Month F-M-A as spring, M-J-J as summer, A-S-O as autumn, and N-D-J as winter). We define M-J-J as summer to consider the early summer maxima of lower tropospheric O_3 (see Sect. 3.3).

The PBL O_3 over Beijing showed a strong diurnal cycle in summer and a much weaker one in winter. In the early morning (05:00–08:00 LT) of summer, O_3 was very low at the surface (~25 ppbv) and had a strong concentration gradient below 1 km. This is a typical O_3 distribution in nocturnal and morning PBL (Kleinman et al., 1994; Hidy, 2000; Cheung and Wang, 2001), which is a combined result of dry deposition, surface uptake, and chemical destruction (e.g. titration of NO) in the stable nocturnal PBL (Logan, 1985; Reiter, 1991; Neu et al., 1994).

After 08:00 LT, the PBL O_3 gradually increased with an annual mean rate of 3~4 ppbv h^{-1} and a much higher summertime rate (6–7 ppbv h^{-1}) in the lower PBL where the precursors were often of very high concentrations. The rapid O_3 increase in the morning has been mainly attributed to downward transport of O_3-rich air mass after the breakup of the nocturnal PBL (Reiter, 1991; Mckendry and Lundgren, 2000; Cheung and Wang, 2001). In the afternoon, the PBL O_3 concentrations reached the daily maximum at 13:00–14:00 LT in summer but at 15:00–16:00 LT on annual average. The afternoon maximum of PBL O_3 is a typical feature downwind of an urban area, and the peak time often depends on the distance from the city (Logan, 1989; Wang et al., 2001, 2005, 2006a). The diurnal variation of MOZAIC O_3 in the lower PBL is similar to those measured in summer 2005 at a mountainous site about 50 km north of the center of Beijing (Wang et al., 2006a).

Since the MOZAIC aircraft routes cover a large area around Beijing (see Fig. 1) the data can thus provide useful information on the spatial-temporal variations of PBL

ACPD
7, 9795–9828, 2007

EGU

O_3. Figures 5a to 5i show the gridded mean summertime O_3 concentrations at different altitudes in the lower troposphere (horizontal resolution: ~4 km; vertical interval: 0.8 km) in early morning (05:00–08:00 LT), later morning (09:00–12:00 LT) and afternoon (13:00–16:00 LT). These figures reveal that high O_3 concentrations generally appeared in northeastern and eastern suburban areas of Beijing in summer. In comparison, frequent O_3 pollution episodes have been observed at the ground level in mountainous areas north of Beijing during summer (Wang et al., 2006a), which has been attributed to mountain-valley breezes transporting urban plumes to the north.

3.3 Seasonal cycles of tropospheric ozone and their causes

3.3.1 Seasonal changes in tropospheric ozone and their relations to meteorological conditions

O_3 throughout the troposphere exhibits a seasonal cycle, and the exact pattern and the underlying causes can vary at different locations (Monks, 2000). In Fig. 6a, we show the seasonal patterns of O_3, pooled from three daytime periods (05:00–08:00 LT, 09:00–12:00 LT and 13:00–16:00 LT), over Beijing at four altitude bins. It can be seen that the O_3 concentrations had a summer maximum and a winter minimum throughout the troposphere: a broad summer maximum (May–August) was observed in the middle troposphere (4 km–8 km); while a sharper early summer peak (in June) was found in the lower troposphere (below 4 km).

A broad summer maximum of O_3 in the middle troposphere has been widely observed in Europe and North America and was mainly attributed to photochemical production (Liu et al., 1987; Logan, 1999; Law et al., 2000; Zbinden et al., 2006). Analysis of data in Japan showed that middle-tropospheric O_3 exhibit a summer maximum in northern Japan and a spring maximum and a summer minimum in the southern parts (Logan, 1989; Austin and Midgley, 1994; Thouret et al., 1998b; Naja and Akimoto, 2004). This phenomenon has been attributed to the influence of the Asian summer monsoons which bring maritime air with low O_3 air from the tropical Pacific to southern

Japan (Logan, 1989; Thouret et al., 1998b). In the interior region of the Asian continent, a summer maximum of O_3 was observed over the northeastern Tibet-Qinghai Plateau (Wang et al., 2006b), which has been attributed to a possible source of stratosphere-to-troposphere exchange (Ding and Wang, 2006). For the broad mid-tropospheric summer maximum of O_3 over Beijing, another important source may be the biomass burnings in Central Asia and Russia (Pochanart et al., 2003; Nedelec et al., 2005; Qin et al., 2006), whose plumes can be rapidly transported to middle and even upper troposphere by warm conveyor belts (Nedelec et al., 2005). We further discuss this issue with trajectory analysis in Sect. 3.3.2.

The June peak of O_3 in the lower troposphere in Beijing is most likely the result of photochemical production from anthropogenic sources. Wang et al. (2001) showed an early summer maxima of surface O_3 (in May) at Lin'an, in central-eastern China just before the rainy season starts in that region, while southern China had an annual maximum in autumn (Lam et al., 2001; Wang et al., 2005). The different seasonal patterns can be explained by distinct meteorological conditions in different parts of China. To learn about the relationship between meteorological conditions and the seasonal patterns of O_3 over Beijing, we examined seasonal variations in monthly mean wind, sunshine hours, and total rainfall measured at the Beijing Observatory during 1995–2005 (Fig. 6b). It shows that the lower tropospheric wind blew more southerly in summer due to the onset of the Asian summer monsoons. The mean daily sunshine hours decreased significantly from June to July and August accompanying a sharp increase in total rainfall, indicating that the monsoons in late summer bring more frequent rainy/cloudy weather conditions to Beijing. The reduced sunlight and increased rainfall in July and August can partially explain the reduced O_3 concentrations in the two month compared to June.

To examine if there was an unusual source of emission contributing to the June O_3 maxima, such as open-field burning of crop residues, we show the monthly mean tropospheric NO_2 column retrieved from GOME and SCIAMACHY satellite for June (Fig. 7a) and August (Fig. 7b), and in Figs. 7c and 7d we also present the ATSR-2 total fire count

maps for the two months. Here we combined the GOME and SCIAMACHY data to calculate the average of the NO_2 column. The same treatment has been adopted by others (e.g. Richter et al., 2005). Inspection of these figures clearly reveals a difference in tropospheric NO_2 column and biomass burning activities between June and August. The very intensive biomass burnings in June were mostly related to the harvest of wheat in the NCPs and East China (Wang et al., 2002). Besides the decreased contribution from the biomass burning emissions, the reducing tropospheric NO_2 column in August could also be attributed to more efficient wet removal processes in August.

Besides photochemical production and removal, long-range transport can also play a role in the seasonal cycle of O_3. To see if the there is a change in the Asian summer monsoons from June to August, in Figs. 8a–d we show the mean geopotential heights and wind streams at 1000 hPa and 850 hPa levels in June and August for 1995–2005. A comparison of Figs. 8a and 8c suggests that the southern, eastern and northern China are dominated by the summer monsoons in both months: in June the surface winds over Beijing were mostly from the south in contrast to a southeasterly wind in August (see marked arrows). At the 850 hPa level, winds came mainly from southwest in June and southeast in August (see Figs. 8b and 8d). The change in the circulations of the Asian monsoon system between the two months can be attributed to the northward movement of sub-tropic High over the Pacific (Ding, 1994), which can also be seen from the geopotential heights given in Figs. 8b and 8d. These results suggest that Beijing was more influenced by regional pollution sources in the polluted NCPs in June. The more frequent impact of maritime air masses in August is the main cause of the cloudy/rainy weather in Beijing.

In summary, favorable meteorological conditions such as stronger solar radiation and a prevailing southerly wind (facilitating transport of regional emissions) and more intensive biomass burning activities in June could be the cause of the narrow seasonal O_3 peak observed in June over Beijing.

3.3.2 The impact of long-range transport on tropospheric O_3 in summer

In this section we use back-trajectory analysis to gain further insights into contributions from different source regions to the O_3 concentrations at different altitudes of the troposphere over Beijing. Only the summer months (M-J-J) of 1997, 1998, and 2005 when there were a large number of data samples, were chosen for this analysis. Three-day 3-D back-trajectories were calculated at 07:00–08:00 LT, 11:00–12:00 LT, and 15:00–16:00 LT on selected days with fine weather conditions according to 3-h surface rainfall data. The endpoints of the trajectories were at 1.2 km, 3 km and 5 km over the airport, representing the upper PBL, the lower free troposphere and the middle troposphere, respectively. All trajectories were ended at the airport, not at exact locations on aircraft routes. In Figs. 9a–c, we show the classified trajectories at the three altitudes. The PBL trajectories was classified into two categories (Fig. 9a): one group (N) was transported from the remote areas in the north with fast wind speeds; the other (S) was originated from the polluted regions in the south with low wind speeds. For the higher altitudes (Figs. 9b and 9c), besides the N and S air-mass types in the PBL, a third air-mass type from west (W) was identified. The vertical tracks of these trajectories, showing as latitude-height plots, are given on the right side of these figures.

Based on the trajectory classifications at the three altitudes, we calculated the mean O_3 profiles for each air-mass group at different vertical layers from surface to 6 km, which are shown in Fig. 10, together with the total number of O_3 profiles in each category. It can be seen that below 2 km the profile number of Type N is smaller than that of Type S, but above 2 km the opposite is true, which indicates that the summer monsoons mainly influence the lower troposphere. Below 2 km, air masses from the south contained higher O_3 concentrations (by 15–20 ppbv) than that from the north with the largest difference occurring at 1 km altitude. This is what one expects to see as the air from the north was less influenced by emissions in the NCPs. Interestingly air masses arriving from the west also contained elevated O_3 concentrations in the lower free troposphere (2–4 km). Inspection of individual trajectories suggests that most of these

west-coming air masses in the lower free troposphere coincided with air from the south in the PBL, suggesting that the NCPs pollution was lifted over the mountains in the northwest of the NCPs and then was carried by the westerlies to the free troposphere over Beijing.

In the free troposphere, the mean O_3 concentrations of Type S decreased significantly and were even lower than those from the north and the west above 4 km. This further reveals that the broad mid-tropospheric summer maximum over Beijing was not caused by anthropogenic emissions convected from the NCPs and the Central-Eastern China, but was due to transport of biomass burning plumes from Central Asia and Russia or due to the upper-tropospheric/stratospheric sources as above discussed. Figure 9 also shows that air masses of N and W often passed over Central Asia and Russia but experienced subsidence before arriving at Beijing, especially in the middle troposphere. However, since the forest fire plumes can also be transported to middle even upper troposphere by warm conveyor belts (Nedelec et al., 2005; Real et al., 2007), it is difficult to determine which source dominated the summertime maximum in the middle troposphere. This topic can be further addressed in the future with the additional synchronous MOZAIC measurements of carbon monoxide (CO) and total reactive nitrogen oxides (NO_y) with O_3 since 2002 (http://mozaic.aero.obs-mip.fr).

3.4 Decadal trend of lower tropospheric O_3 over Beijing

With a rapid industrialization and urbanization, emissions of ozone precursors in China are thought to have increased significantly (Richter et al., 2005). So far there has been no published result on the long-term trend of O_3 on the Chinese subcontinent. Here we use MOZAIC data to attempt to derive a decadal tendency of lower tropospheric O_3 over Beijing.

Because the number of MOZAIC samples in some years like 2000–2001 are too few to calculate the annual average, we made use of the data obtained during two periods, 1995–1999 and 2000–2005, to study the decadal trend. Figure 11 shows the vertical O_3 profiles for the two periods averaged over year-round data and over summer after-

noons only (LT 15:00–16:00, May–July). It can be seen that the mean O_3 level in lower troposphere has increased substantially in the last decade in Beijing. The difference is about 5–8 ppbv in the PBL with the largest increase at 1 km altitude. Considering 1997 and 2004 as the middle of the two periods(see Fig. 1b), the annual change rate is about 1 ppbv yr^{-1}, or about 2% for a mean level of 50 ppbv. For summer afternoons, a much larger increase (up to 22 ppbv) was found in the PBL with an increase rate of about 3 ppbv yr^{-1} (or ~4% for a mean level of 75 ppbv). In contrast, the mean O_3 concentrations in the free troposphere have not shown such an increase. The large increase in O_3 in the boundary layer in Beijing is in sharp contrast to the situation in Paris, New York City, and Tokyo. Figure 12 shows the mean O_3 profiles during the same period for those three cities, which shows constant O_3 levels throughout the troposphere in the last decade.

To see if there exists a relationship between the observed O_3 increase over Beijing and changes in emissions of NO_2, an O_3 precursor, in Fig. 13 we show GOME and SCIAMACHY retrieved tropospheric NO_2 column in the NCPs (see dashed line box in Fig. 7) and around Beijing (1×1° box centered at 116.5° N, 40° E), together with the total number of civilian vehicles in Beijing City (http://www.stats.gov.cn/tjsj/ndsj/) from 1996 to 2005. It can be seen that in the last decade both regional (NCPs) and Beijing urban emissions of NO_x have sharply increased, particularly in urban Beijing (with a rate up to 23% yr^{-1}), and the latter correlated very well with a rapid increase in the total number of civilian vehicles in Beijing (28% yr^{-1}). These results strongly suggest that increasing anthropogenic emissions have enhanced tropospheric O_3 over Beijing and possibly in other cities as well.

4 Conclusions

In this work we analyzed O_3 data collected by the MOZAIC program from 1995 to 2005 and provided a first climatology of tropospheric O_3 over Beijing and the surrounding areas. O_3 over Beijing shows a similar vertical distribution to other northern mid-latitude

locations, but has higher daytime O_3 concentrations (up to 10 ppbv) in the lower troposphere than other mega-cities of similar latitudes. O_3 exhibits a narrow early summer peak in June in the lower troposphere and a broad summer maximum in the middle troposphere. The June peak in the lower troposphere was attributed to favorable meteorological conditions conducive to photochemical production of O_3 and transport of regional pollution and also to more intense biomass burning activities in the North China Plains. The broad mid-tropospheric summer maximum is on the other hand mostly likely due to stratosphere-troposphere exchange or transport of forest burning plumes in Central-Asia and Russia.

Different from Tokyo, New York City, and Paris, which had a stable or declining trend in tropospheric O_3 during the past decade, the daytime O_3 concentrations in the lower troposphere over Beijing have increased at a rate up to 2% yr^{-1}. This increasing trend is believed to be a result of increased anthropogenic emissions in Beijing and the surrounding areas. More research and management efforts are needed to address the high (and increasing) O_3 concentrations in Beijing.

Acknowledgements. This work was funded by Hong Kong Research Grant Council (Project PolyU5144/04E), National Basic Research Program of China ('973 Project No.2005CB422203), and The Hong Kong Polytechnic University (Project 1-BB94). The authors acknowledge for the strong support of the European Commission, Airbus, and the Airlines (Lufthansa, Austrian, Air France) who carry free of charge the MOZAIC equipment and perform the maintenance since 1994. MOZAIC is presently funded by INSU-CNRS (Institut National des Sciences de l'Univers – Centre National de la Recherche Scientifique, France), Météo-France, and FZJ (Forschungszentrum Jülich, Germany). The Final Analysis Data (FNL) and HYSPLIT model were obtained from NOAA CDC and NOAA ARL, respectively. Surface meteorological data were provided by the Data Support Section of the Computation and Information Systems Laboratory at the National Center for Atmospheric Research. GOME and SCIAMACHY data were provided by ESA through TEMIS.

References

Akimoto, H., Nakane, H., and Matsumoto, Y.: The chemistry of oxidant generation: tropospheric ozone increase in Japan, Chemistry of the Atmosphere: The Impact on Global Change, edited by: Calvert, J., Blackwell Scientific Publications, Oxford, UK, 261–273, 1994. 9797

Akimoto, H.,and Narita, H.: Distribution of SO_2, NO_x, and CO_2 emissions from fuel combustion and industrial activities in Asia with $1^\circ \times 1^\circ$ resolution, Atmos. Environ., 28(2), 213–225, 1994. 9797

Austin, J. F. and Midgley, R. P.: The climatology of the jet-stream and stratospheric intrusions of ozone over Japan, Atmos. Environ., 28(1), 39–52,1994. 9804

Beekmann, M. Ancellet, G., and Megie, G.: Climatology of tropospheric ozone in southern Europe and its relation to potential vorticity, J. Geophys. Res., 99, 12 841–12 853, 1994. 9797, 9802

Bojkov, R. D.: Ozone changes at the surface and in the free troposphere, in: Tropospheric Ozone: Regional and Global Scale Interactions, edited by: Isaksen, I. S. A., and Reidel, D., 83–96, Dordrecht, Netherlands, 1988. 9797

Chan, C. Y., Chan, L. Y., Chang, W. L., Zheng, Y. G., Cui, H., Zheng, X. D., Qin, Y., and Li, Y. S.: Characteristics of a tropospheric ozone profile and implications for the origin of ozone over subtropical China in the spring of 2001, J. Geophys. Res., 108(D20), 8800, doi:10.1029/2003JD003427, 2003. 9798

Cheung, V. T. F. and Wang, T.: Observational study of ozone pollution in rural site in the Yangtze Delta of China, Atmos. Environ., 35, 4947–4958, 2001. 9797, 9803

Cooper, O. R., Stohl, A., Eckhardt, S., Parrish, D. D., Oltmans, S. J., Johnson, B. J., Nedelec, P., Schmidlin, F. J., Newchurch, M. J., Kondo, Y., and Kita, K.: A springtime comparison of tropospheric ozone and transport pathways on the east and west coasts of the United States, J. Geophys. Res., 110, D05S90, doi:10.1029/2004JD005183, 2005. 9802

Crutzen, P. J: A discussion of the chemistry of some minor constituents of the stratosphere and troposphere, Pure Appl. Geophys., 106–108, 1385–1399, 1973. 9797

Ding, A. and Wang, T.: Influence of stratosphere-to-troposphere exchange on the seasonal cycle of surface ozone at Mount Waliguan in western China, Geophys. Res. Lett., 33(3), L03803, doi:10.1029/2005GL024760, 2006. 9805

Ding, Y.: Monsoons Over China, Kluwer Acd., Norwell, Mass., 420pp., 1994. 9806

Fishman, J., Ramanathan, V., Crutzen, P. J., and Liu, S. C.: Tropospheric ozone and climate,

Nature, 282, 818–820, 1979. 9797
Fishman, J., Wozniak, A. E., and Creilson, J. K.: Global distribution of tropospheric ozone from satellite measurements using the empirically corrected tropospheric ozone residual technique: Identification of the regional aspects of air pollution, Atmos. Chem. Phys., 3, 893–907, 2003, http://www.atmos-chem-phys.net/3/893/2003/. 9798, 9802
Gao, J., Wang, T., Ding, A. J., and Liu, C.: Observation study of ozone and carbon monoxide at the summit of mount Tai (1534 m a.s.l.) in central-eastern China, Atmos. Environ., 39, 4779–4791, 2005. 9797
Hidy, G. M.: Ozone process insights from field experiments Part I: Overview, Atmos. Environ., 34, 2001–2022, 2000. 9803
Kleinman, L., Lee, Y.-N., Springston, S. R., Nunnermacker, L., and Zhou, X. L.: Ozone formation at a rural site in the southeastern United States, J. Geophys. Res., 99, 3469–3482, 1994. 9803
Lam, K. S., Wang, T. J., Chan, L. Y., Wang, T., and Harris, J.: Flow patterns influencing the seasonal behaviors of surface ozone and carbon monoxide at a coastal site near Hong Kong, Atmos. Environ., 35, 3121–3135, 2001. 9797, 9805
Law, K. S., Plantevin, P. H., Thouret, V., Marenco, A., Asman, W. A. H., Lawrence, M., Crutzen, P. J., Muller, J. F., Hauglustaine, D. A., and Kanakidou, M.: Comparison between global chemistry transport model results and Measurement of Ozone and Water Vapor by Airbus In-Service Aircraft (MOZAIC) data, J. Geophys. Res., 105(D1), 1503–1525, 2000. 9804
Liu, J., Zhang, X. L., Zhang, X. C., and Tang, J.: Surface ozone characteristics and the correlated factors at Shangdianzi atmospheric background monitoring station, Research of Environmental Sciences (in Chinese), 19(4), 19–25, 2006. 9797
Liu, S. C., Trainer, M., Fehsenfeld, F. C., Parrish, D. D., Williams, E. J., Fahey, D. W., Hubler, G., and Murphy, P. C.: Ozone production in the rural troposphere and the implications for regional and global ozone production, J. Geophys. Res., 92, 4191–5207, 1987. 9797, 9804
Logan, J. A.: Tropospheric ozone: seasonal behavior trends, and anthropogenic influence. J. Geophys. Res., D6, 10 463–10 482, 1985. 9797, 9803
Logan, J. A.: Ozone in rural areas of the United States, J. Geophys. Res., 94, 8511–8532, 1989. 9803, 9804, 9805
Logan, J. A.: Trends in the vertical distribution of ozone: An analysis of ozonesonde data, J. Geophys. Res., 99, 25, 553–25, 585, 1994. 9797, 9802

Logan, J. A.: An analysis of ozonesonde data for the troposphere: Recommendations for testing 3-D models and development of a gridded climatology for tropospheric ozone, J. Geophys. Res., 104(D13), 16 115–16 149, 1999. 9804
Luo, C, John, J. C. S., Zhou, X. J., Lam, K. S., Wang, T., and Chameides, W. L.:A nonurban ozone air pollution eipsode over eastern China: Observations and model simulations, J. Geophys. Res., 105(D2), 1889–1908, 2000. 9797
Marenco, A., Thouret, V., Nedelec, P., Smit, H., Helten, M., Kley, D., Karcher, F., Simon, P., Law, K., Pyle, J., Poschmann, G., Wrede, R. V., Hume, C., and Cook, T: Measurement of ozone and water vapor by Airbus in-service aircraft: The MOZAIC airborne program, An overview, J. Geophys. Res., 103(D19), 25 631–25 642, 1998. 9799
McKee, D. J.: Tropospheric ozone: human health and agricultural impacts, Lewis Publishers, New York, 9–18, 1994. 9797
McKendry, I. G. and Lundgren, J.: Tropospheric layering of ozone in regions of urbanized complex and/or coastal terrain: a review, Prog. Phys. Geog., 24, 3, 329–354, 2000. 9803
Monks, P. S.: A review of the observations and origins of the spring ozone maximum, Atmos. Environ., 34, 3545–3561, 2000. 9797, 9804
Naja, M., and Akimoto H.: Contribution of regional pollution and long-range transport to the Asia – Pacific Region: Analysis of long-term ozonesonde data over Japan, J. Geophys. Res., 109, D21306, doi:10.1029/2004JD004687,2004. 9804
Nedelec, P., Thouret, V., Biroude, J., Sauvage, B., Cammas, J.-P., and Stohl, A.: Extreme CO concentrations in the upper troposphere over the northeast Asia in June 2003 from the in situ MOZAIC aircraft data, Geophys. Res. Lett. 32, L14807, doi:10.1029/2005GL023141, 2005. 9805, 9808
Neu, U., Kunzle, T., and Wanner, H.: On the relation between ozone storage in the residual layer and daily variation in near-surface ozone concentration – a case study, Bound. Lay. Meteorol., 69, 221–247, 1994. 9803
NRC (National Research Council): Rethinking the Ozone Problem in Urban and Regional Air Pollution, National Academy Press, Washington, D.C., 1991. 9797
Oltmans, S. J., Lefohn, A. S., Scheel, H. E., Harris, J. M., Levy II, H., Galbally, I. E., Brunke, E. G., Meyer, C. P., Lathrop, J. A., Johnson, B. J., Shadwick, D. S., Cuevas, E., Schmidlin, F. J., Tarasick, D. W., Claude, H., Kerr, J. B., Uchino, O., and Mohnen, V.: Trends of ozone in the troposphere, Geophys. Res. Lett., 25, 139–142, 1998. 9797
Pochanart, P., Akimoto, H., Kinjo, Y., and Tanimoto, H.: Surface ozone at four remote island

sites and the preliminary assessment of the exceedances of its critical level in Japan, Atmos. Environ., 36, 4235–4250, 2002. 9797
Pochanart, P., Akimoto, H., Kajii, Y., Potemkin, V. M., and Khodzher, T. V.: Regional background ozone and carbon monoxide variations in remote Siberia/East Asia, J. Geophy. Res., 108(D1), 4028, doi:10.1029/2001JD001412, 2003. 9805
Qin, S. G., Ding, A. J., and Wang, T.: Transport pattern of biomass burnings air masses in Eurasia and the impacts on China, China Environment Science, 26(6), 641–645, 2006. 9805
Real, E., Law, K. S., Weinzierl, B., Fiebig, M., Petzold, A., Wild, O., Methven, J., Arnold, S., Stohl, A., Huntrieser, H., Roiger, A., Schlager, H., Stewart, D., Avery, M., Sachse, G., Browell, E., Ferrare, R., and Blake, D.: Processes influencing ozone levels in Alaskan forest fire plumes during long-range transport over the North Atlantic, J. Geophys. Res., 112, D10S41, doi:10.1029/2006JD007576, 2007. 9808
Reiter, R.: On the mean daily and seasonal variations of the vertical ozone profiles in the lower troposphere, Atmos. Environ., 25A, 1751–57, 1991. 9803
Richter, A., Burrows, J. P., Nub, H., Granier, C., and Niemeier, U.: Increase in tropospheric nitrogen dioxide over China observed from space, Nature, 437, 129–132, 2005. 9797, 9806, 9808
Shao, M., Tang, X. Y., Zhang, Y. H., and Li, W. J.: City clusters in China: air and surface water pollution, Frontiers in Ecology and the Environment, 4(7), 353–361, 2006. 9798
Streets, D. G., Bond T. C., Carmichael, G. R., Fernandes, S. D., Fu, Q., He, D., Klimont, Z., Nelson, S. M., Tsai, N. Y., Wang, M. Q., Woo, J. H., and Yarber, K. F.: An inventory of gaseous and primary aerosol emissions in Asia in the year 2000, J. Geophys. Res., 108(D21), 8809, doi:10.1029/2002JD003093, 2003. 9797
Taylor, J. K. and Cihon, C.: Statistical Techniques for data analysis, Second Edition, Chapman and Hall/CRC, 2004. 9801
Thouret, V., Marenco, A., Nedelec, P., and Grouhel, C.: Ozone climatologies at 9–12 km altitude as seen by the MOZAIC airborne program between September 1994 and August 1996, J. Geophys. Res., 103(D19), 25 653–25 679, 1998a. 9799
Thouret, V., Marenco, A., Logan, J. A., Nedelec, P., and Grouhel, C.: Comparison of ozone measurements from the MOZAIC airborne program and the ozone sounding network at eight locations, J. Geophys. Res., 103(D19), 25 695–25 720, 1998b. 9800, 9802, 9804, 9805
Thouret, V., Cammas, J. P., Sauvage, B., Athier, G., Zbinden, R., Nedelec, P., Simon, P., and Karcher, F.: Tropopause referenced ozone climatology and inter-annual variability (1994–

2003) from the MOZAIC programme, Atmos. Chem. Phys., 6, 1033–1051, 2006, http://www.atmos-chem-phys.net/6/1033/2006/. 9799

Wang, T., Cheung, T. F., Anson, M., and Li, Y. S.: Ozone and related gaseous pollutants in the boundary layer of eastern China: Overview of the recent measurements at a rural site, Geophys. Res. Lett., 28, 2373–2376, 2001. 9797, 9803, 9805

Wang, T., Cheung, T. F., Li, Y. S., Yu, X. M., and Blake, D. R.: Emission characteristics of CO, NO_x, SO_2 and indications of biomass burning observed at a rural site in eastern China, J. Geophys. Res., 107, 4157–4167, 2002. 9806

Wang, T., Ding, A. J., Gao., J., and Wu, W. S.: Strong ozone production in urban plumes from Beijing, China, Geophys. Res. Lett., 33(21), L21806, doi:10.1029/2006GL027689, 2006a. 9797, 9798, 9803, 9804

Wang, T., Guo, H., Blake, D. R., Kwok, Y. H., Simpson, I. J., and Li, Y. S.: Measurements of trace gases in the inflow of South China Sea background air and outflow of regional pollution at Tai'O, Southern China, J. Atmos. Chem., 52(3), 295–317, 2005. 9797, 9803, 9805

Wang, T. and Kwok, J. Y. H.: Measurement and analysis of a multiday photochemical smoge episode in the Pearl River Delta of China, J. Appl. Meteorol., 42, 404–416, 2003. 9797

Wang, T., Wong, H. L. A., Tang, J., Ding, A., Wu, W. S., and Zhang, X. C.: On the origin of surface ozone and reactive nitrogen observed at a remote mountain site in the northeastern Qinhai-Tibetan Plateau, western China, J. Geophys. Res., 111, D08303, doi:10.1029/2005JD006527, 2006b. 9805

Xu, X. B., Lin, W. L., Wang, T., Yan, P., Tang, J., Meng, Z. Y., and Wang, Y.: Enhanced variability of surface ozone at a regional background station in eastern China 1991–2006, Geophys. Res. Lett., unpublished results, 2007. 9797

Zbinden, R. M., Cammas, J. P., Thouret, V., Nedelec, P., Karcher, F., and Simon, P.: Mid-latitude tropospheric ozone columns from the MOZAIC program: climatology and inter-annual variability, Atmos. Chem. Phys., 6, 1053–1073, 2006, http://www.atmos-chem-phys.net/6/1053/2006/. 9804

Zheng, X. D., Zhou, X. J., Tang, J., Qin, Y., and Chan, C. Y.: A meteorological analysis on a low tropospheric ozone event over Xining, North Western China on 26–27 July 1996, Atmos. Environ., 38(2), 261–271, 2004. 9798

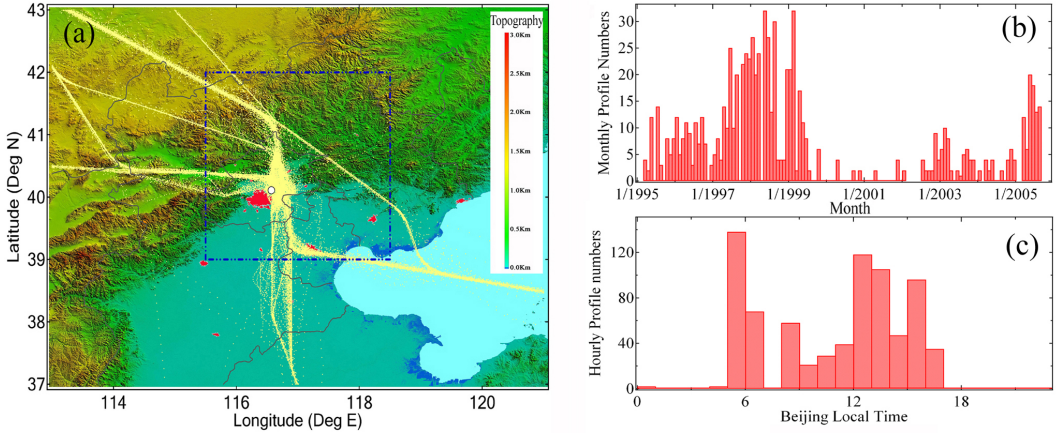

Fig. 1. **(a)** Geographical coverage of the MOZAIC flight routes around Beijing during 1995–2005, presented on topographical map with urban area colored red, and distributions of the total number of vertical profiles as a function of **(b)** month, and **(c)** of the time of day. The legend in Fig. 1a shows the scale of terrain.

ACPD
7, 9795–9828, 2007

EGU

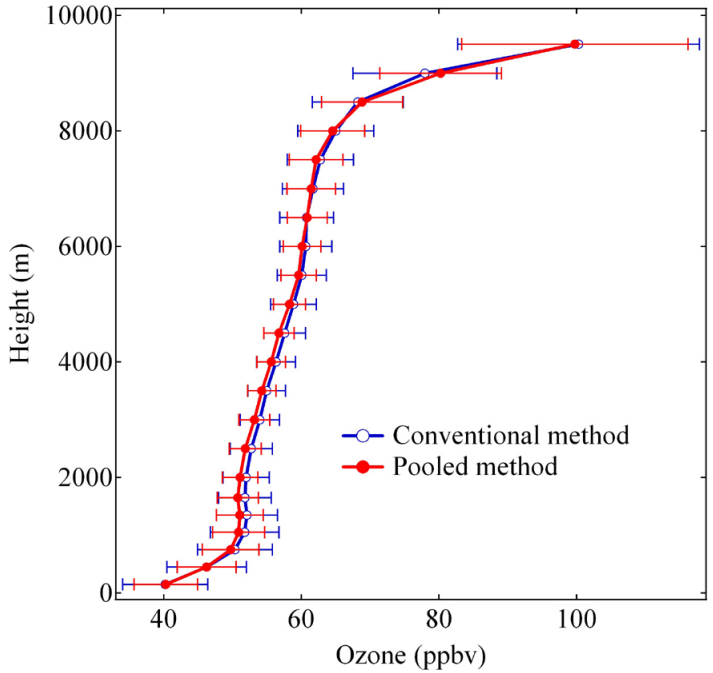

Fig. 2. Distributions of tropospheric O_3 (Mean±0.5sd or ±0.5S_p, same in other figures) over Beijing using conventional and pooled statistical methods.

ACPD
7, 9795–9828, 2007

EGU

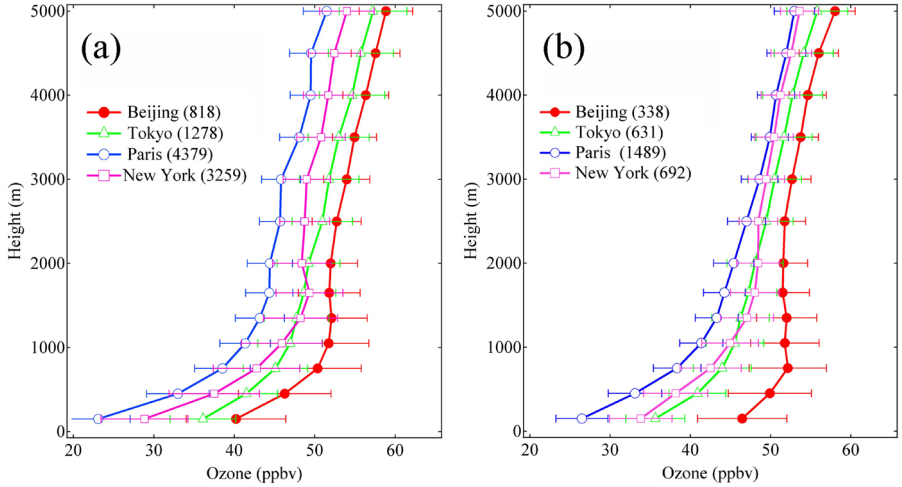

Fig. 3. Comparison of O_3 distributions in low troposphere over Beijing (39.9° N), Tokyo (35.7° N), Paris (48.8° N), and New York City (40.7° N), using **(a)** conventional average with all data and **(b)** pooled method with data recorded between 10:00–14:00 LT. The total number of valid profiles used in statistics for each city is given in the parentheses.

ACPD
7, 9795–9828, 2007

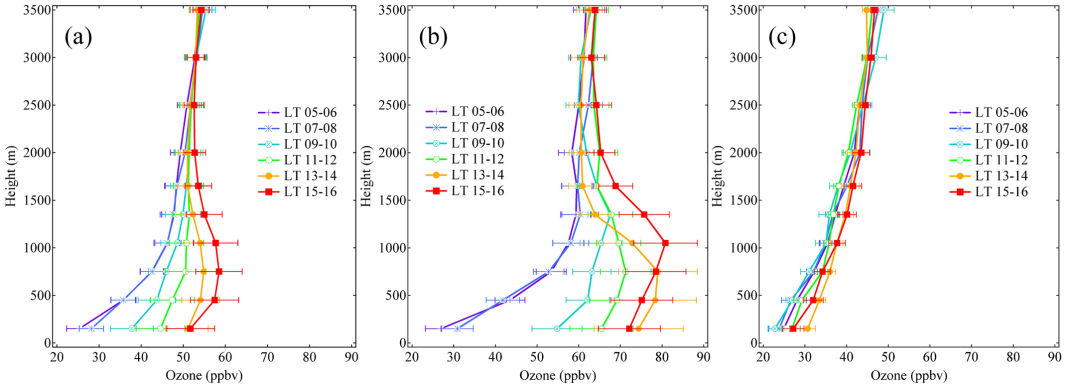

Fig. 4. Diurnal patterns of O_3 profiles for **(a)** annual average, **(b)** summer (MJJ), and **(c)** winter (NDJ) in the lower troposphere.

ACPD
7, 9795–9828, 2007

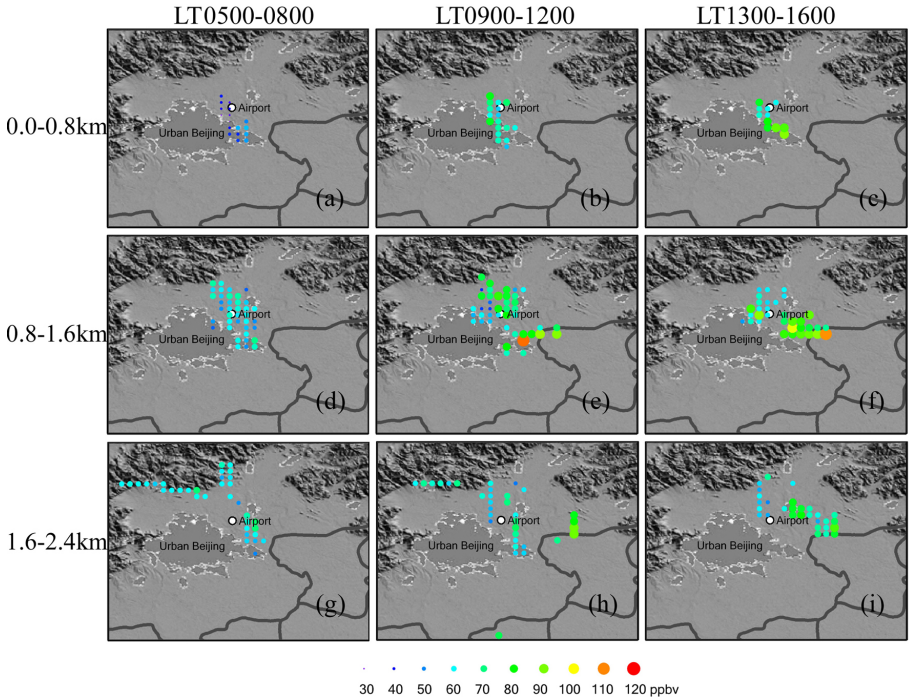

Fig. 5. Horizontal distributions of mean O_3 concentrations around Beijing at different altitudes of the lower troposphere for different daytime periods in summer (MJJ).

ACPD
7, 9795–9828, 2007

EGU

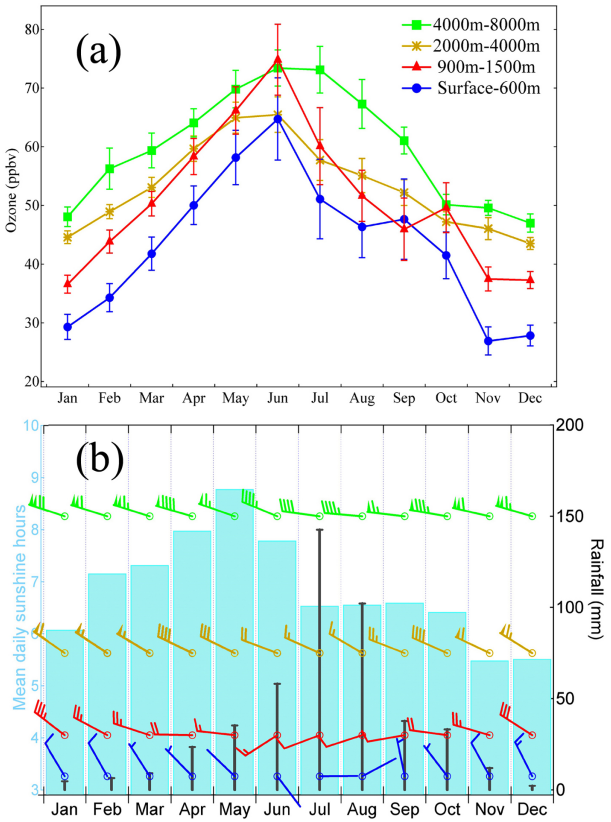

Fig. 6. Seasonal variations of **(a)** O_3 concentrations at different tropospheric levels over Beijing, and of **(b)** wind profiles, mean sunshine hours and monthly total rainfall at Beijing.

ACPD
7, 9795–9828, 2007

EGU

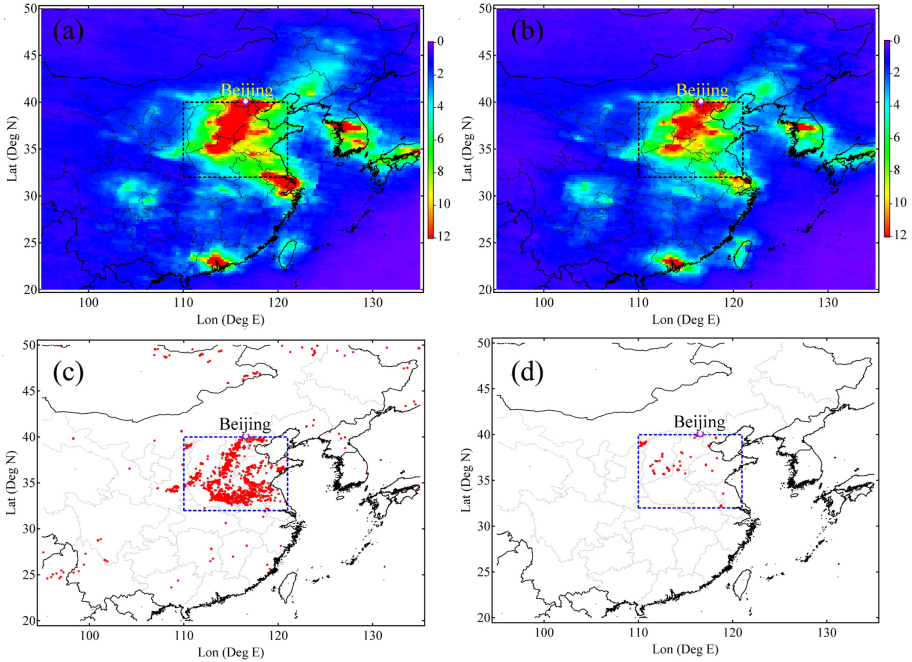

Fig. 7. Climatology of tropospheric NO_2 column retrieved from GOME (1995–2002) and SCIAMACHY (2003–2005) satellite data in **(a)** June and **(b)** August during 1995–2005, and ATSR-2 total fire count map in **(c)** June and **(d)** August during 1996–2005.

ACPD
7, 9795–9828, 2007

EGU

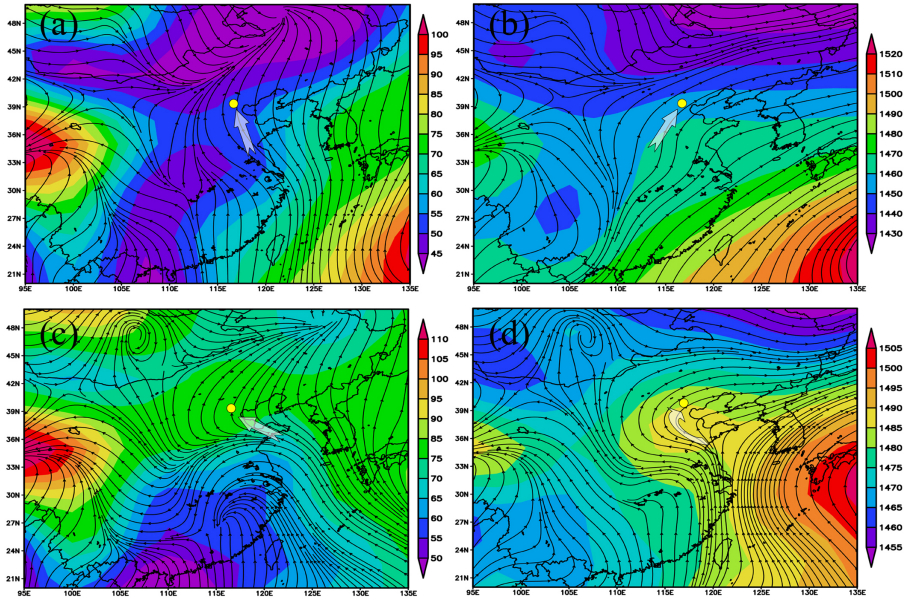

Fig. 8. Monthly mean geopotential heights and wind streams, **(a)** at 1000 hPa in June, **(b)** at 850 hPa in June, **(c)** at 1000 hPa in August, and **(d)** at 850 hPa in August, during 1995–2005.

ACPD
7, 9795–9828, 2007

EGU

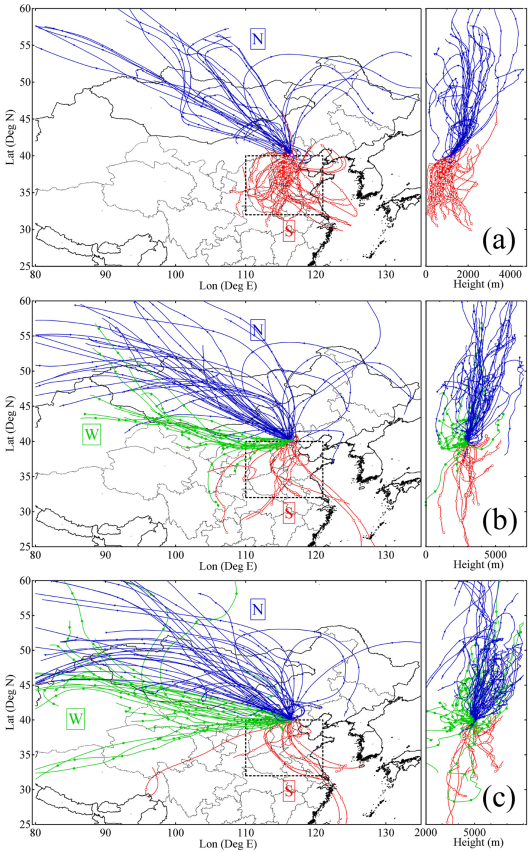

Fig. 9. Clusters of 3-day back-trajectories ending at **(a)** 1.2 km, **(b)** 3 km, and **(c)** 5 km over Beijing during May-July in 1997, 1998 and 2005. The right side parts of these figures show the vertical locations of trajectories as a function of latitude.

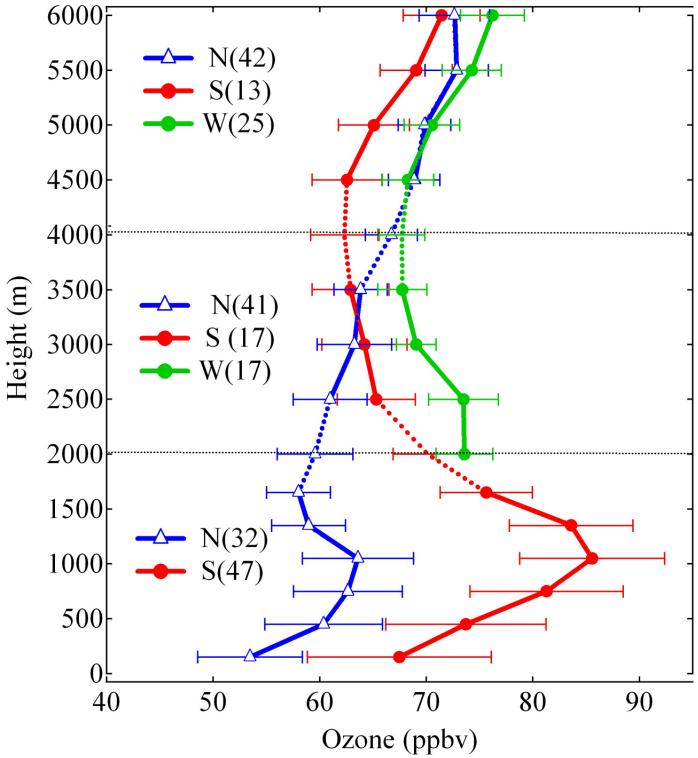

Fig. 10. Mean O_3 distributions of different air mass types based on trajectory cluster analysis in the PBL (0–2 km),in lower free troposphere (2–4 km) and in the middle troposphere (4–6 km) over Beijing. Profile number of each category is given in the parentheses.

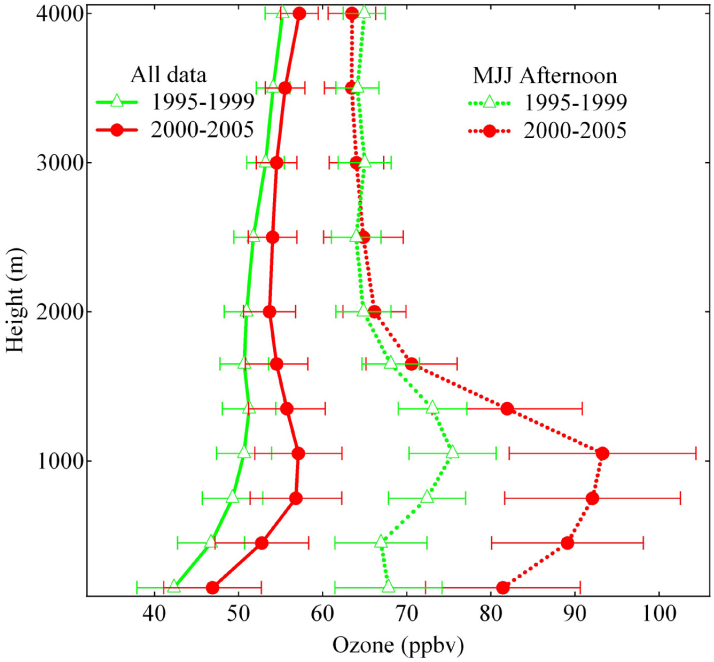

Fig. 11. Comparisons of mean O_3 profiles in the lower troposphere over Beijing between 1995–1999 and 2000–2005. The real lines are annual mean values, and the dashed lines on the right side represent the data collect in summer afternoon (at LT 15:00–16:00 in MJJ).

ACPD
7, 9795–9828, 2007

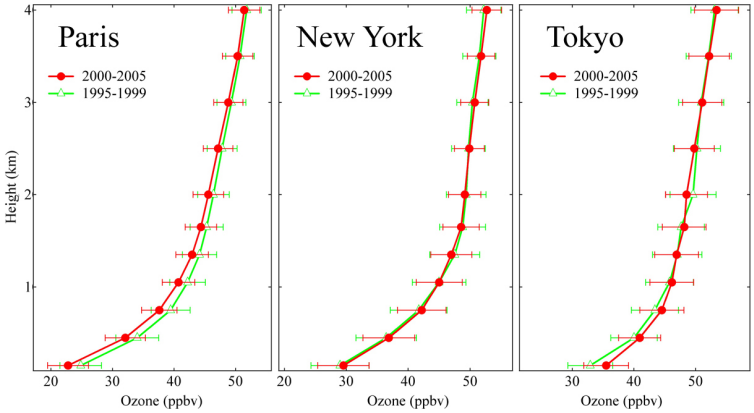

Fig. 12. Comparisons of annual mean O_3 profiles between 1995–1999 and 2000–2005 in the lower troposphere over Paris, New York City, and Tokyo.

ACPD
7, 9795–9828, 2007

EGU

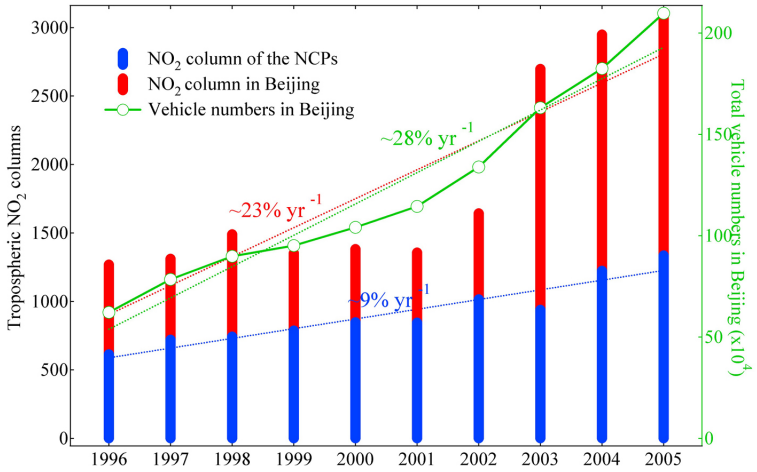

Fig. 13. Trends of annual mean tropospheric NO_2 columns (Unit: $1e^{13}$ molecules/cm^2) in the NCPs and Beijing (data from GOME and SCIAMACHY), and annual total numbers of civilian vehicles in Beijing (Data from Chinese Statistical Yearbook 1996–2006).